The Impacts of AMMA Radiosonde Data on the French Global Assimilation and Forecast System

C. Faccani, Florence Rabier, Nadia Fourrié, A. Agusti-Panareda, Fatima Karbou, Patrick Moll, Jean-Philippe Lafore, Mathieu Nuret, F. Hdidou, Olivier Bock

The Impacts of AMMA Radiosonde Data on the French Global Assimilation and Forecast System

C. FACCANI, F. RABIER, AND N. FOURRIÉ

CNRM-GAME, Météo-France, and CNRS, Toulouse, France

A. AGUSTI-PANAREDA

ECMWF, Reading, United Kingdom

F. KARBOU, P. MOLL, J.-P. LAFORE, AND M. NURET

CNRM-GAME, Météo-France, and CNRS, Toulouse, France

F. HDIDOU

Direction de la Météorologie Nationale, Casablanca, Morocco

O. BOCK

Laboratoire de Recherche en Géodésie, IGN, Marne La Vallée, France

(Manuscript received 1 December 2008, in final form 20 March 2009)

ABSTRACT

The high vertical density soundings recorded during the 2006 African Monsoon Multidisciplinary Analysis (AMMA) campaign are assimilated into the French numerical weather prediction Action de Recherche Petite Echelle Grande Echelle (ARPEGE) four-dimensional variational data assimilation (4DVAR) system, with and without a bias correction for relative humidity. Four different experiments are carried out to assess the impacts of the added observations. The analyses and forecasts from these different scenarios are evaluated over western Africa. For the full experiment using all data together with a bias correction, the humidity analysis is in better agreement with surface observations and independent GPS observations than it was for the other experiments. AMMA data also improve the African easterly jet (AEJ) on its southeasterly side, and when they are used with an appropriate bias correction, the daily and monthly averaged precipitation results are in relatively good agreement with the satellite-based precipitation estimates. Forecast scores are computed with respect to surface observations, radiosondes, and analyses from the European Centre for Medium-Range Weather Forecasts (ECMWF). The positive impacts of additional radiosonde observations (with a relevant bias correction) are found to propagate downstream with a positive impact over Europe at the 2–3-day forecast range.

1. Introduction

The African Monsoon Multidisciplinary Analysis (AMMA) is an international project focused on the study of the African monsoon (Redelsperger et al. 2006). Rainfall changes during this particular period of the year are important to the people living in the monsoon areas. As a matter of fact, over the last few decades, West Africa experienced abundant rainfall during the 1950s and 1960s, and very dry conditions between the 1970s and 1990s. The environmental and socioeconomical impacts of these dramatic changes are devastating for western African populations who lead a rural life (e.g., Sultan et al. 2005; Milesi et al. 2005).

To better understand the mechanisms of the African monsoon and to prevent dramatic situations in the future, the AMMA project has been developed on different nested time scales of observations and analysis periods, from one year to a decade. The 1-yr period of enhanced observations (special observation period) took

Corresponding author address: Florence Rabier, CNRM-GAME, Meteopole, 42 Av. Coriolis, Toulouse 31057, France.
E-mail: florence.rabier@meteo.fr

DOI: 10.1175/2009WAF2222237.1

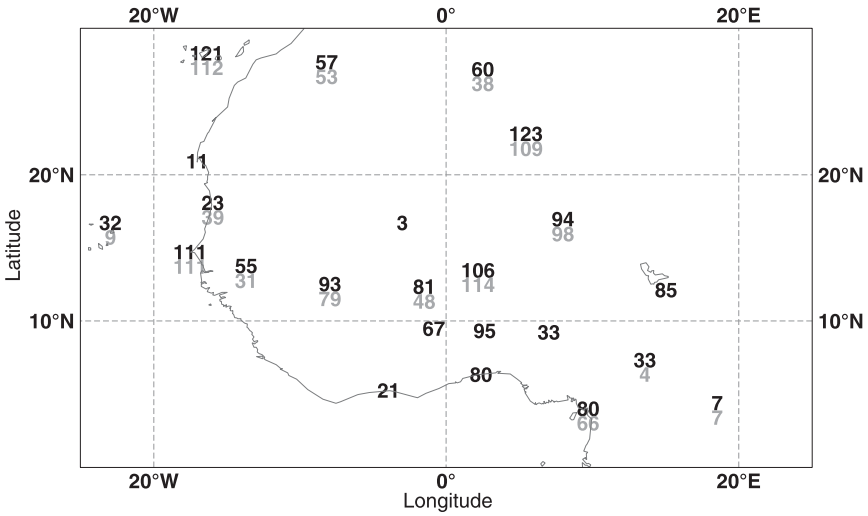

FIG. 1. Distribution of the radiosonde network over western Africa. The numbers of soundings provided by each GTS station available at Météo-France at 0000 and 1200 UTC during the period 15 Jul–15 Sep 2006 (2005) are indicated in black (gray).

place in 2006 from the beginning of the year (dry phase) to the onset and the penetration of the monsoon into the African continent. Some intensive observation periods (IOPs) were selected in order to investigate the physical and dynamical processes of the monsoon. For this purpose, the observation network over western Africa has been reorganized and improved (Parker et al. 2008). Specific areas of interest have been selected and provided with observation stations, such as radars, dropsondes, GPS antennas, and radiosondes. The reorganization of the observation network mainly concerned the radiosonde network, which, before AMMA, had only a few operating stations in the World Meteorological Organization (WMO) Global Telecommunication System (GTS). Radiosonde data are an extremely important source of information over land for weather forecast models, because they provide the assimilation procedure with a complete description of the three-dimensional structure of the atmosphere. Other available data, such as satellite radiances, provide indirect information about the atmospheric temperature and humidity structure with a relatively coarse vertical resolution, compared to radiosonde profiles. Furthermore, they are more difficult to use over land than over sea and, as a consequence, are only partially used over land. Only high-peaking channels, describing the stratosphere and upper troposphere, are generally assimilated. Information about the lower troposphere is then lacking from satellite data over the African continent. Although radiosonde observations do not suffer from these limitations, they come at a significant cost, which explains why their coverage is limited. Not only is the cost of maintaining these observation stations relatively high for poor countries, but there is often no adequate communication network for transmitting the data.

As a result of the efforts deployed during AMMA, the 2006 radiosonde network was composed of 24 fully operational stations, a few of them providing 3-hourly data, for a total of around 7000 soundings during the period June–September 2006. Twenty-one of these stations are still operational, whereas the others were used only for the 2006 campaign. For an extensive and complete description of the AMMA contribution to the establishment of the African radiosonde network, see Parker et al. (2008).

This large amount of additional radiosonde data is expected to have positive impacts on the weather forecasts over western Africa. In this paper, the influences of the number of radiosonde sites, the relevance of vertical high-resolution soundings, and the effects of a humidity bias correction are assessed.

The paper is organized as follows. Sections 2 and 3 of this paper describe the data processing and the model setup. The results of the assimilation diagnostics and forecast performance are discussed, respectively, in sections 4 and 5. Conclusions are presented in section 6.

2. Data processing

Figure 1 shows the distribution of the western African GTS radiosonde network sites in 2006 (black) and in 2005 (gray), and the number of soundings valid at 0000 and 1200 UTC and received at Météo-France from 15 July to 15 September. Figure 1 shows that for 2006 there were five new stations along the Guinea gulf (bottom

of the domain) and inland (N'Djamena, Chad, 12.08°N, 15.02°E, with 85 soundings), as well as an increased level of activity for most of the preexisting stations. In fact, during the period under consideration (mid-July–mid-September 2006), special soundings were taken in order to monitor the diurnal cycle of the monsoon, which was particularly intense (Parker et al. 2005). Therefore, during the 2006 IOPs, a large number of radiosondes, including the new ones, were launched several (up to 8) times per day. For a detailed description of the activity of the radiosonde network in 2006, see Parker et al. (2008).

All data recorded during the AMMA campaigns are collected and stored, as raw measurements, in a common database (information online at http://database.amma-international.org). Radiosonde data are stored in their original form, that is, with a vertical resolution, on average, 10 times finer than a World Meteorological Organization (WMO) standard sounding. Due to the increased number of launches per day, several soundings coming from the same station are available in the 6-h window used for data assimilation (next section). Moreover, the large number of vertical levels allows for a better description of the vertical structure of the atmosphere, which is extremely important for an accurate description of the monsoon evolution patterns over these regions. In particular, radiosonde data are an important source of moisture data, a crucial piece of information that enables the study of the thermodynamical processes in the atmosphere. For these reasons, several studies have been conducted in order to detect and to quantify the errors associated with the relative humidity from radiosondes. It is well known (Lorenc et al. 1996; Wang et al. 2002) that several radiosonde types have a dry bias, and specific studies (Bock et al. 2007; Agusti-Panareda and Beljaars 2008) focusing on the radiosondes used during the AMMA campaign confirmed the existence of a dry bias in the data. The reasons of these errors can be explained by many factors such as contamination of the packaging material (sonde type RS80-A), sonde age (Roy et al. 2004), storage conditions (RS80-A), and solar heating (sonde type RS92) among others. Nuret et al. (2008) proposes a humidity bias correction scheme, which is a function of temperature and humidity, for the Vaisala RS80-A, which is affected by a strong dry bias. Agusti-Panareda et al. (2009) estimate the bias correction as a function of relative humidity (RH), solar elevation angle, sonde type, and vertical pressure using radiosondes over western Africa. Thus, they have developed correction functions for many radiosonde types (Vaisala RS80-A, Vaisala RS92, and MODEM). Since several types of radiosondes were used during the 2006 AMMA campaign, and since the Nuret et al. (2008) method has to date only been performed on the Vaisala RS80-A, the Agusti-Panareda et al. (2009) scheme was preferred for this study. In fact, their approach gives a bias correction for all radiosonde types over our area of interest. The humidity correction is a linear combination of four sine waves (Fourier transforms) calculated by matching the cumulative distribution functions (CDFs) of the RH observations and their model equivalents from short-range forecasts [see Agusti-Panareda et al. (2009) for details]. Only humidity data of radiosondes located between the equator and 20°N are corrected (observations from 19 out of the 24 AMMA radiosonde network sites are affected).

3. Model setup

The French numerical weather prediction (NWP) system is developed in collaboration with the European Centre for Medium-Range Weather Forecasts (ECMWF; Courtier et al. 1991). A four-dimensional variational data assimilation (4DVAR; Courtier et al. 1994; Veersé and Thépaut 1998; Rabier et al. 2000) approach is used for data assimilation, with a 6-h assimilation window. A modified version of the French global model Action de Recherche Petite Echelle Grande Echelle (ARPEGE), which was operational in 2007, was used in this study. This particular configuration of ARPEGE 4DVAR (Gauthier and Thépaut 2001; Janisková et al. 1999) has 46 vertical levels up to 10 Pa with a spectral truncation of T358, which gives a horizontal resolution on the order of 50 km over western Africa. Conventional observations such as radiosonde or surface data are operationally assimilated into ARPEGE 4DVAR. Radiosonde temperature data are corrected with functions depending on the sonde type and the solar elevation, similarly to the bias correction previously used at ECMWF (Bouttier et al. 1999). Clear-sky radiances from satellite instruments [e.g., the High Resolution Infrared Radiation Sounder (HIRS), the Advanced Microwave Sounding Unit (AMSU-A and -B), and the Special Sensor Microwave Imager (SSM/I)] and retrieved quantities (wind) from other satellite instruments [e.g., the Geostationary Operational Environmental Satellite (GOES) and Meteosat], together with some surface winds from the Quick Scatterometer (QuikSCAT), are also assimilated (information is available for each of the instruments online at http://www.wmo.int/pages/prog/sat/). The background matrix used to quantify the short-range forecast errors in the data assimilation process is estimated using the ensemble method of Berre et al. (2006). The modification to the operational configuration is in the calculation of the land surface emissivity ϵ for AMSU-A and AMSU-B, in order to increase the number of assimilated radiance observations used over land.

TABLE 1. Assimilation experiments: name, use of radiosonde data, and use of bias correction for humidity.

Expt	Description	RHbc
CNTR	GTS data in 2006	No
AMMA	GTS data in 2006, AMMA special soundings	No
AMMABC	GTS data in 2006, AMMA special soundings	Yes
PREAMMA	GTS data in 2005	No
NOAMMA	No AMMA soundings	No

The operational model emissivity is based on Grody (1998) or Weng et al. (2001), which provides a fixed value or a statistical estimation of ϵ. The new approach is described by Karbou et al. (2006), and its aim is to obtain a more realistic estimation of the surface land emissivity, with a retrieval based on physical parameters (such as surface temperature and atmospheric transmission). An evaluation of the positive impacts of this new approach on weather forecasts is described in Karbou et al. (2009a). This version of the model is used as a basis for our experiments.

During AMMA, slightly more than half of the program's radiosonde profiles were transmitted in real time via the GTS, in WMO format [i.e., only with mandatory and wind–temperature at significant levels]. The AMMA database, on the other hand, has collected all of the radiosonde profiles at high vertical resolution, even if they were not transmitted in real time. A control experiment (CNTR) has been run with all of the radiosoundings that were available on the GTS at the time. Four additional experiments were performed to test the sensitivity to the AMMA special soundings (Table 1).

The first experiment, called AMMA, is similar to the CNTR configuration, but it also includes the additional soundings and the multilevel soundings from the AMMA database (in particular, the low-resolution soundings sent via the GTS are substituted for the corresponding multilevel ones). This experiment is intended to test the impacts of using additional AMMA data that were not available in real time. Another experiment (AMMABC) is similar to AMMA, but in this case the Agusti-Panareda et al. (2009) bias correction for relative humidity described in section 2 is applied. This experiment will then document the changes brought about by a bias correction of the data. Two other experiments were run with degraded radiosonde networks, as data denial reference experiments. PREAMMA is similar to CNTR, but with a degraded radiosonde network (only stations in gray in Fig. 1 are assimilated). This experiment will then be representative of what the analyses would have been if the AMMA project had not existed. NOAMMA is an additional experiment that was run to represent an extreme reference. It does not include any data from the 24 sondes constituting the AMMA radiosonde network.

Most of the experiments were run for the 2-month period of 15 July–15 September 2006, except for NOAMMA, which was run for the 45-day period of 1 August–15 September 2006. ARPEGE 4DVAR is cycled through the period and a 4-day forecast is started at 0000 UTC each day, for each experiment. The first 15 days of assimilation are sometimes discarded in the diagnostics, as they correspond to a warming-up phase. The analysis of the results mostly focuses on the month of August as this is the period of largest activity by the monsoon.

4. Differences in the assimilation

The analyses of the various experiments have been compared with respect to the radiosonde data. In addition, the impacts of the assimilation of the different observation sets have been studied for the humidity and the wind fields.

a. Comparisons with radiosonde data

The various experiments use very different amounts of radiosonde data over the African region. In particular, one can compare the data used by the CNTR and AMMA experiments. The former uses data received operationally via the GTS in 2006, while the latter uses all available data from the AMMA database. Statistical results are presented in Fig. 2 over the whole African area to the north of the equator. The number of observations is indicated in the columns in the middle of Fig. 2. The number of observations used in AMMA is indicated in black, while the difference between the number of observations used in AMMA and in CNTR is indicated in gray. One can see that there are many more observations available in AMMA (up to 5 times more). Statistics of differences between the analysis–background and radiosonde data were also computed for both experiments and are shown in Fig. 2. These differences are computed at each analysis time for the whole period and averaged over the whole period. The arithmetic average of the differences (observation − model) is shown in the right-hand panels (named BIAS). The root-mean square (RMS) of the differences (observation − model) is shown in the left-hand panels. The statistics related to background (analysis) fields are shown as solid (dashed) lines. The increase in the number of observations when going from CNTR to AMMA is not detrimental to the statistics of the fit of the model to the observations. On the contrary, an improvement in the RMS of the background (solid line) is observed for AMMA (black) for

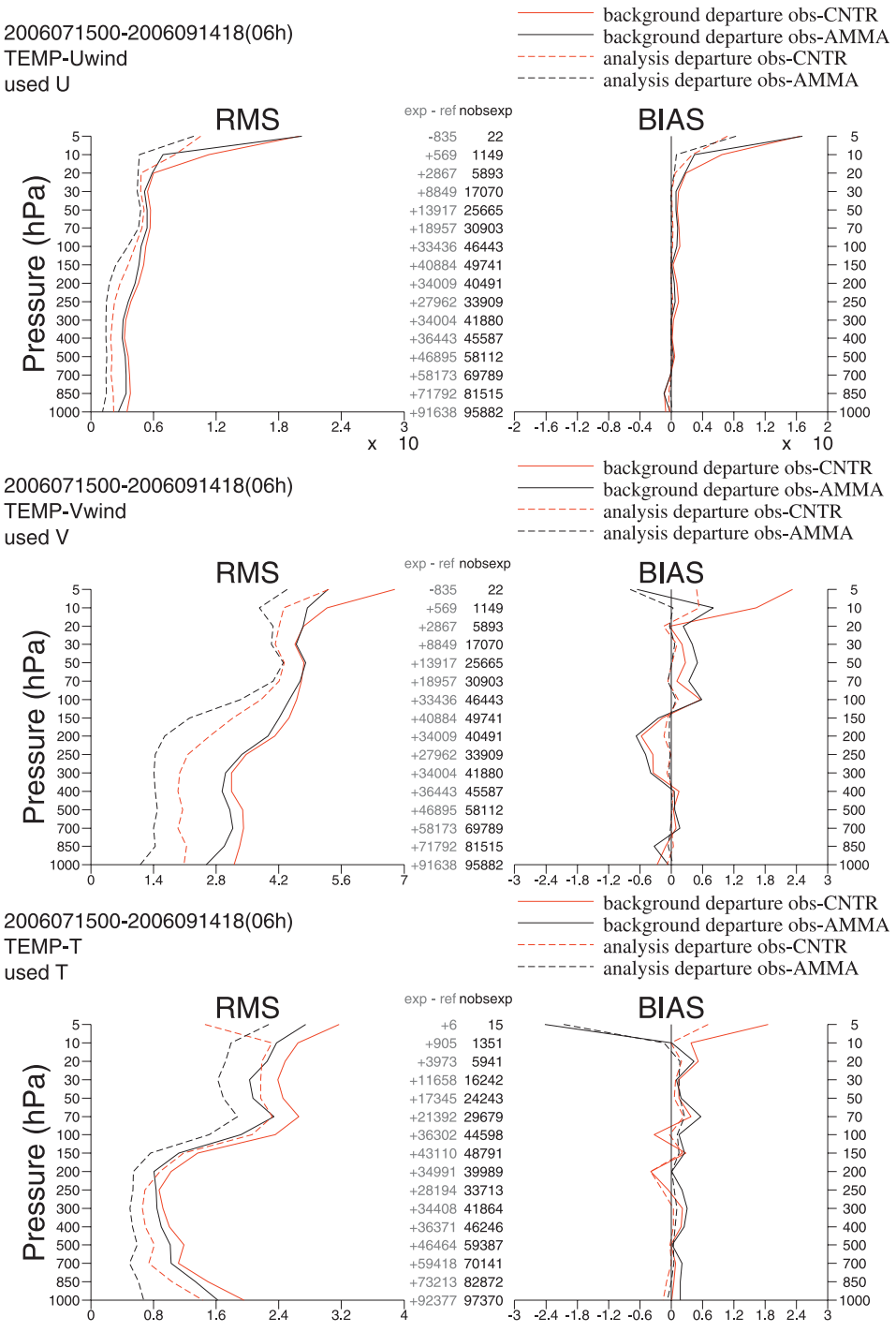

FIG. 2. RMS and mean (BIAS) of the differences between the analysis (dashed lines)–background (solid lines) and radiosonde observations for experiments AMMA (black) and CNTR (red) as a function of pressure. Shown are the results for (top) *U*, (middle) *V*, and (bottom) *T*. The numbers printed in the middle indicate the number of observations used (black for the number of data points used in the AMMA experiment and gray for the difference between the number of data points used in the AMMA and the CNTR experiments). Statistics are calculated over the whole African region to the north of the equator and averaged over 2 months.

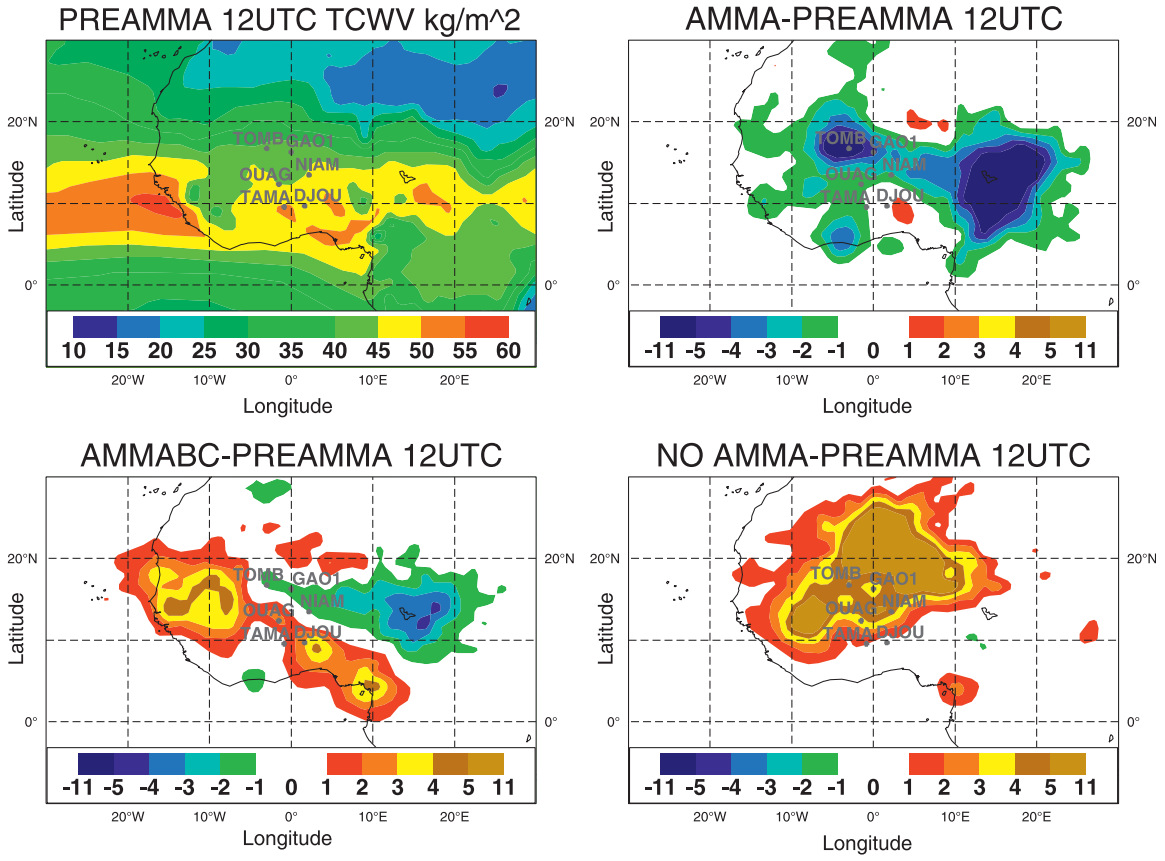

FIG. 3. The 45-day-averaged TCWV at 1200 UTC for (top left) PREAMMA, and the differences between (top right) AMMA and PREAMMA, (bottom left) AMMABC and PREAMMA, and (bottom right) NOAMMA and PREAMMA. See Table 1 for a description of the experiments. The averaging period is from 1 Aug to 14 Sep 2006. Locations of GPS measurements are indicated with the first letters of the names of the stations.

both the horizontal wind component (Fig. 2, top and middle) and the temperature (Fig. 2, bottom). The improvement is larger for V than for U, and is larger in the lower troposphere than in the stratosphere. The changes in temperature extend to the whole atmosphere, with the largest impact seen in the stratosphere. Negligible impact on the AMMA experiment is observed for the specific humidity (not shown), while AMMABC only shows an improvement on the lower troposphere (up to 850 hPa, not shown).

A quantification of the changes produced in the humidity field by using the special AMMA campaign soundings can be seen when looking at the total-column water vapor. Figure 3 shows the mean total-column water vapor (TCWV) over the period 1 August–14 September 2006 for the PREAMMA experiment, and the differences that result from the other experiments. PREAMMA (Fig. 3, top left) shows a large area of high water vapor (orange and red) over the Atlantic Ocean and across the western African coast. Several areas of high water vapor content (yellow and orange) are localized inland and along the Sahel. The impacts of the assimilation of AMMA soundings are computed from the difference in AMMA–PREAMMA. The addition of the AMMA soundings produces a widespread decrease of the TCWV inland (Fig. 3, top right), with a large impact on the eastern side. The humidity bias correction (Fig. 3, bottom left) removes the dry bias of the radiosonde data, providing the model with more water vapor than is found in the PREAMMA experiment. It can be noted that the moistening over western Africa is similar to that obtained by Karbou et al. (2009b) when additional satellite data were inserted into the assimilation. Large areas of increased TCWV are observed along the western African coast, central Nigeria, and the Mount Cameroon area mainly as a result of the bias correction applied to the strongly biased RS80-A data. NOAMMA presents a large area of increased water vapor, compared to PREAMMA, but it is inland and away from the coast (Fig. 3, bottom right). Interpreting this difference another way, one can say that the assimilation of the PREAMMA radiosonde data has the effect of drying

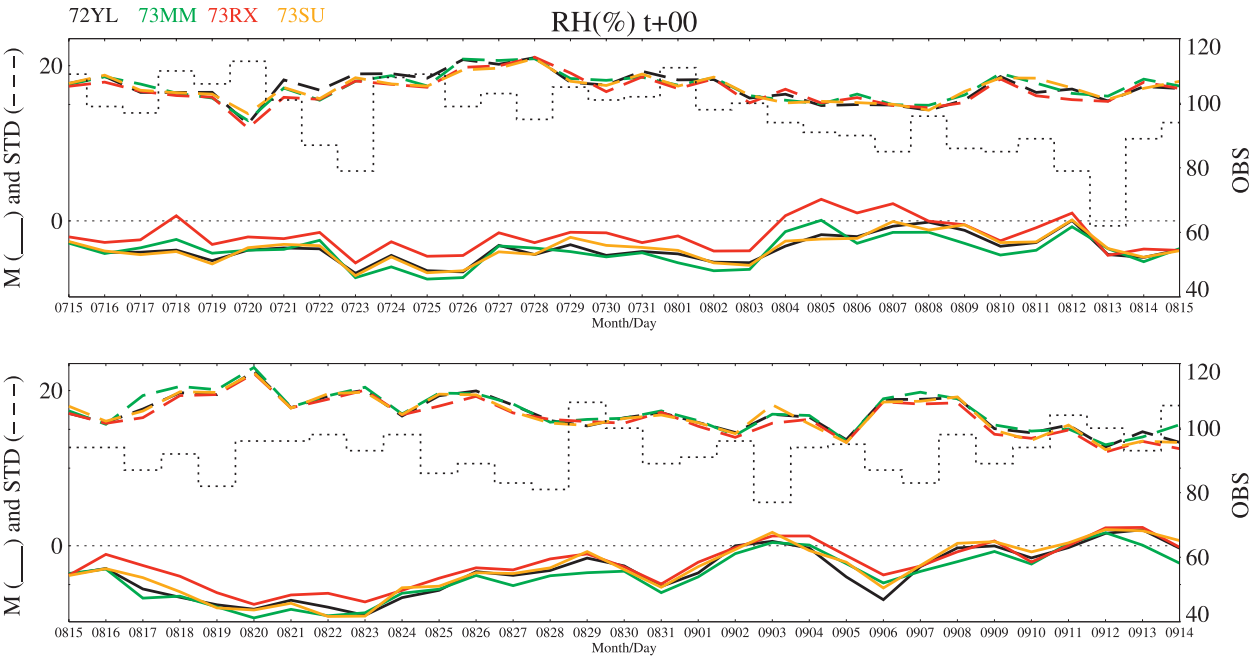

FIG. 4. Mean (M) and std dev (STD) of the difference between the analyses and (SYNOP) surface observations of RH (%) from 15 Jul to 13 Sep 2006. Statistics are calculated over the entire African region to the north of the equator. The color code is black for CNTR, green for AMMA, red for AMMABC, and yellow for PREAMMA. Std devs are shown as dashed lines, and means as solid lines. The numbers of observations used for verification are indicated to the right.

the atmosphere over the region. The assimilation of AMMA radiosonde data on top of these PREAMMA data contributes to an additional drying of the atmosphere (Fig. 3, top right). This drying from the data might be partially balanced by the bias correction (Fig. 3, bottom left). The radiosonde distribution in 2005 (Fig. 1) suggests that the new stations added for the 2006 AMMA campaign strongly drive the moisture transport in ARPEGE. Unfortunately, no monthly averaged observations of the water vapor are available to validate these results, and only an indirect evaluation can be made from independent local observations.

Figure 4 shows the evolution of the mean and standard deviation of the differences between analyses and surface synoptic observations (SYNOPs) for relative humidity over the African area to the north of the equator from 15 July to 13 September 2006. The impacts of the various configurations on RH are quite small, except for the impact brought about by AMMABC. One can see in Fig. 4 that, during the 2-month period of investigation, AMMABC (red) reduces the (dry) bias and the standard deviation for RH, compared to the other configurations. This impact is significant at the 95% level as measured by a Student's t test. This positive impact on RH is larger during the first month (Fig. 4, top) and it becomes more negligible by the end of August (Fig. 4, bottom). The positive impacts of the bias correction on RH are also observed in the forecast up to $t + 72$ (see section 5), even if they are less impactful. These results clearly point out that there is a bias in the data, which can actually inhibit the improvement brought about by these observations on the analysis; however, if or when this bias is resolved, beneficial impacts from additional observations will be realized.

TABLE 2. Mean values of TCWV for the GPS observations and the analysis fields at the six observation locations. The averaging is performed over the period 1 Aug–14 Sep 2006.

	Timbuktu	Niamey	Ouagadougou	Gao	Tamale	Djougou
GPS	41.71	47.39	47.50	41.36	50.04	46.89
CNTRL	40.99	46.38	46.75	42.31	50.49	50.26
AMMA	37.26	46.11	47.05	40.39	50.54	50.81
AMMABC	41.42	46.77	48.71	42.45	51.49	51.57
PREAMMA	41.24	46.39	46.66	42.75	50.19	48.33
NOAMMA	45.62	49.53	49.21	47.14	51.05	48.79

TABLE 3. Correlation between TCWV analysis fields and GPS data at the six observation locations. The averaging is performed for both daily values and 6-hourly values (shown in parentheses) over the period 1 Aug–14 Sep 2006.

	Timbuktu	Niamey	Ouagadougou	Gao	Tamale	Djougou
CNTRL	0.79 (0.72)	0.93 (0.86)	0.83 (0.67)	0.81 (0.72)	0.86 (0.75)	0.87 (0.62)
AMMA	0.89 (0.75)	0.92 (0.85)	0.85 (0.71)	0.84 (0.75)	0.91 (0.73)	0.86 (0.58)
AMMABC	0.89 (0.77)	0.95 (0.88)	0.87 (0.75)	0.82 (0.75)	0.90 (0.79)	0.90 (0.73)
PREAMMA	0.76 (0.67)	0.90 (0.82)	0.73 (0.65)	0.80 (0.71)	0.74 (0.67)	0.79 (0.64)
NOAMMA	0.52 (0.44)	0.66 (0.55)	0.68 (0.62)	0.56 (0.52)	0.64 (0.59)	0.67 (0.52)

Six GPS stations operating throughout West Africa during August 2006 were used as another source of independent measurements to evaluate our analyses of TCWV [see Fig. 3 for the locations of the GPS stations, and Bock et al. (2008) for a description of the use of the network]. Analysis fields are integrated over $0.5° \times 0.5°$ boxes and are compared with these ground-based measurements to evaluate the TCWV variability tendencies in our analyses. The comparisons have been performed using 45 days of GPS measurements (24 hourly observations per day). For each experiment and for each GPS station, the four closest grid points to the GPS station have been determined to calculate an averaged TCWV from the analyses. Table 2 shows mean estimates of TCWV from GPS and from all of the 4DVAR experiments. The results show that the comparison with GPS measurements is generally in favor of AMMABC. The NOAMMA experiment has a systematic moist bias in TCWV for the six GPS stations, whereas the AMMA experiment has a dry bias for the three stations of Timbuktu and Gao in Mali and Niamey in Niger. These results are in good agreement with the differences obtained in Fig. 3 with the PREAMMA experiment. These GPS stations are in fact located in the difference maxima. This is confirmed by Table 3, which shows the correlations between the analyses and the measurements. These were calculated both for daily values and 6-hourly values. Although the correlations are usually better for daily values, the main results are confirmed. It is clear that AMMABC is in good agreement with GPS observations whereas NOAMMA is systematically worse than all of the other experiments. An additional analysis of the results at Niamey and Timbuktu is given in Figs. 5 and 6. In these figures, TCWV daily time series from

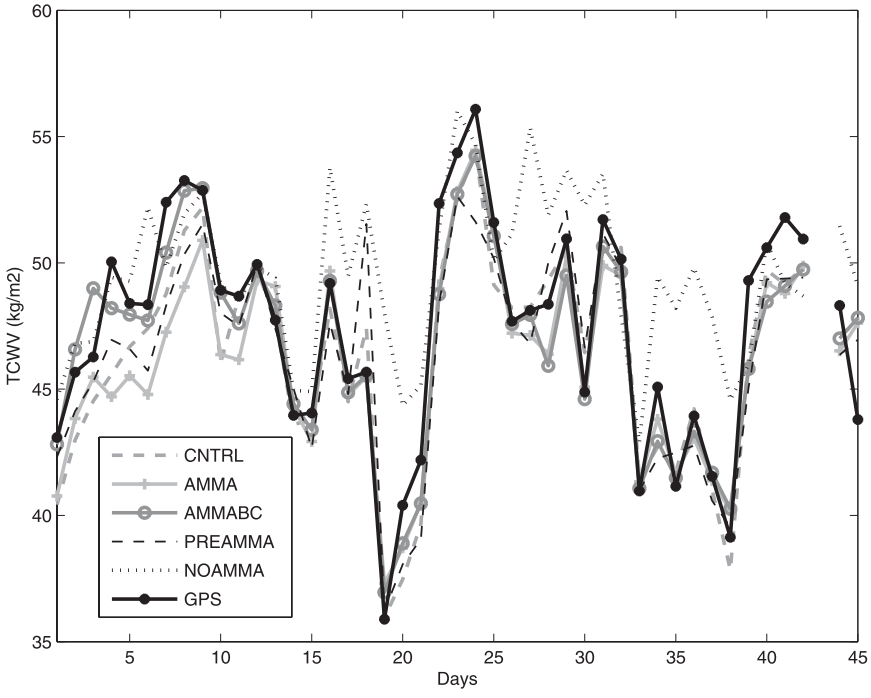

FIG. 5. Daily averages of analyses and GPS observations at Niamey from 1 Aug to 14 Sep 2006. Note that not enough observations were available on 12 September to compare with GPS observations, and, accordingly, values were not plotted for that date.

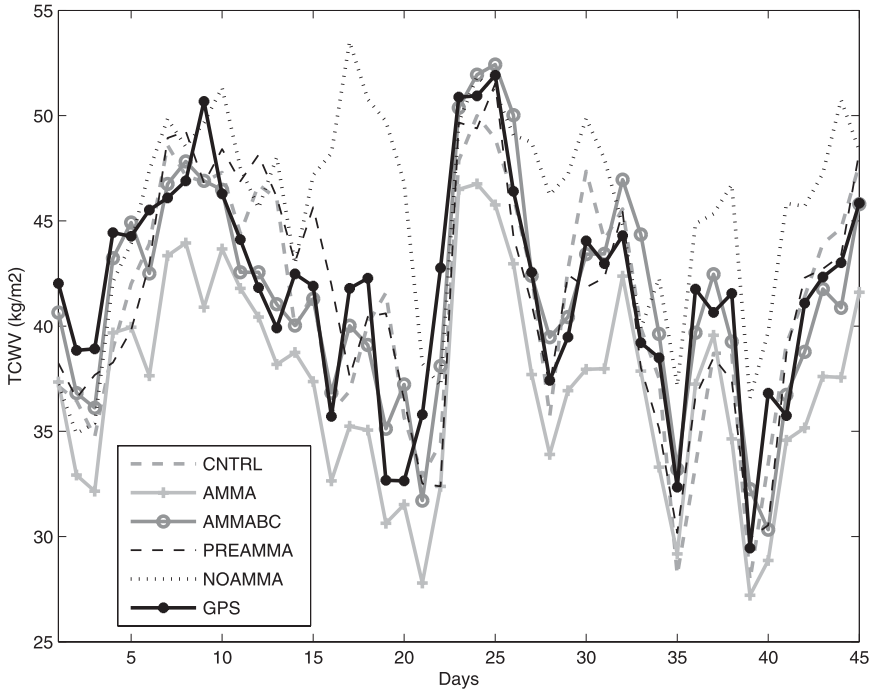

FIG. 6. Daily averages of analyses and GPS observations at Timbuktu from 1 Aug to 14 Sep 2006.

GPS are compared with the TCWV from the various experiments. The time series show how close the TCWV results from the various experiments are to ground-based measurements, except for the NOAMMA experiment, which clearly misrepresents the time evolution of TCWV. Among the other experiments, AMMABC stands out as the experiment best fitting the GPS measurements. At Niamey station, for the first 10 days of the period, AMMABC seems to adjust the TCWV better compared with AMMA. We found the same adjustment of the AMMABC TCWV to GPS measurements for Timbuktu for the whole 45-day period compared to AMMA. This fact suggests, once more that, once the bias present in the data is removed, the analysis will be improved.

b. Impact on the wind field

It is also interesting to study the changes in the wind field, particularly at the level of the African easterly jet (AEJ). It is found that the AEJ changes if the configuration of the radiosonde network is changed. Figure 7 presents the lower boundary of the AEJ (i.e., the zonal wind at 700 hPa). Differences between AMMA and PREAMMA (Fig. 7, top right) show an increase in the AEJ on the southeastern side of the domain. The results are similar for the difference between AMMABC and PREAMMA (Fig. 7, bottom left), whereas NOAMMA (Fig. 7, bottom right) shows a decrease in the AEJ in the middle of the domain. Figure 1 shows that before AMMA there were radiosonde observations only over the Sahel region along the AEJ axis. AMMA brought radiosonde data to the south, allowing us to capture the AEJ extension to the south. The spatial extent to the southeast of the AEJ with the AMMA and AMMABC experiments is interesting because Leroux and Hall (2009) have shown that the African easterly waves (AEWs) triggered by convection are stronger when the AEJ is extended to the south. This might then have an influence on the downstream propagation.

5. Impact on forecasts

a. Impact on rain forecasts

The changes induced into the moisture and wind fields turn into changes in the precipitation fields. The 24-h accumulated precipitation from 0600 to 0600 UTC the next day and averaged over the month of August 2006 shows that CNTR (Fig. 8, top left) produces high rainfall maxima (from cyan to blue) only over the sea. Only light precipitation (up to 12 mm) is observed inland, along the Sahel, mainly close to the Guinea Gulf. The inclusion of high-density vertical level soundings (Fig. 8, top right and middle left) increases the precipitation along the Sahel, especially if a humidity bias correction is applied (Fig. 8, middle left). The PREAMMA experiment (Fig. 8, middle right) exhibits a maximum of precipitation farther to the

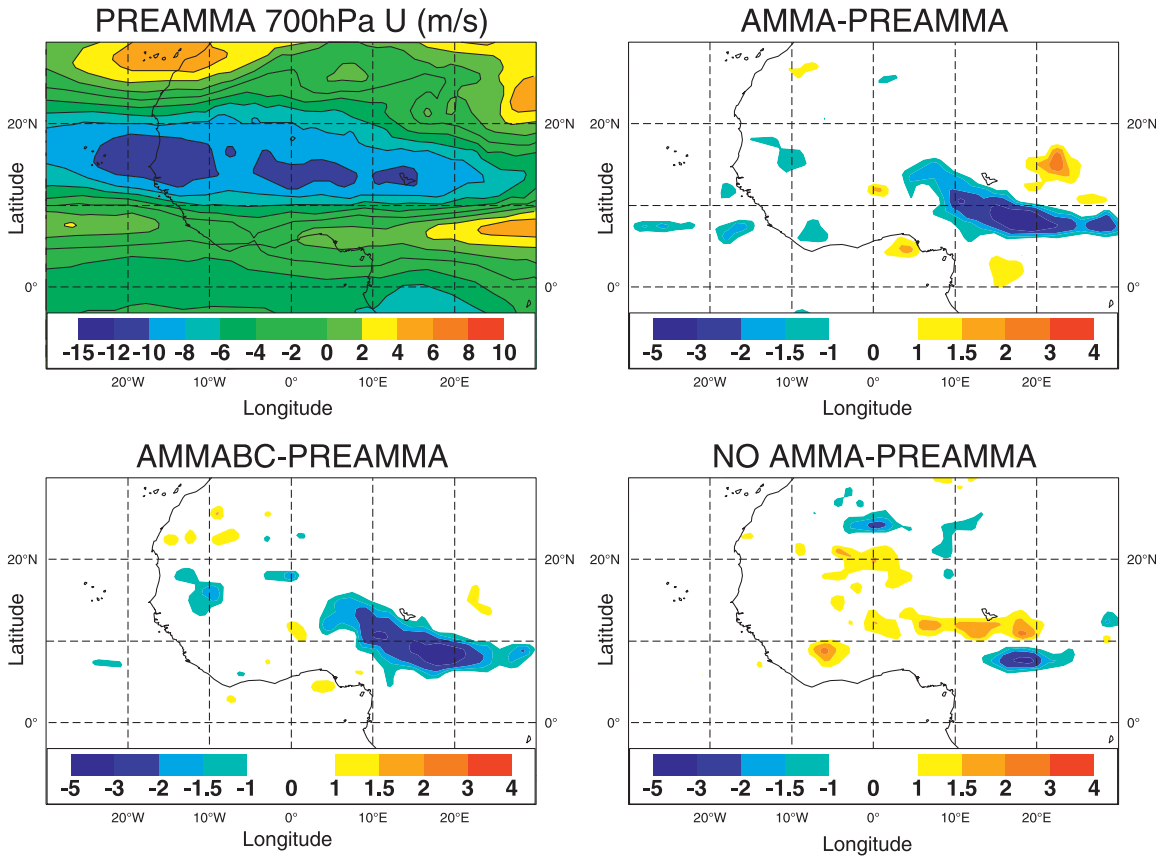

FIG. 7. The 700-hPa zonal wind (m s^{-1}) averaged over the period 1 Aug–14 Sep, at 1200 UTC, for (top left) PREAMMA, and the differences between (top right) AMMA and PREAMMA, (bottom left) AMMABC and PREAMMA, and (bottom right) NOAMMA and PREAMMA.

east than do the other experiments. The NOAMMA experiment does not produce high maxima of precipitation but extends the monsoon higher in latitude in the central part of West Africa. The evaluation of these results is performed against rainfall estimates from the National Oceanic and Atmospheric Administration/Climate Prediction Center's (NOAA/CPC) Famine Early Warning Systems Network (FEWS NET) based on satellite and rain gauge data (Laws et al. 2004). These observations are shown in Fig. 8 (bottom right). The observations prove that all experiments overestimate precipitation over the sea. The maxima (blue) of precipitation observed inland, close to the Guinea Gulf, are reproduced only by AMMABC (forest green), even if they are underestimated. Both PREAMMA and AMMABC seem to correctly forecast the horizontal extent of the inland precipitation area, on the eastern side, in agreement with the positive increments of TCWV (Fig. 3).

Scores have been computed for quantitative precipitation forecasts with respect to the same CPC reference dataset. For this quantitative precipitation comparison, all precipitation fields have been averaged in 100 km × 100 km boxes. Figure 9 shows values of the equitable threat score (ETSs) for the various analysis experiments and the various precipitation thresholds. The NOAMMA experiment is clearly not performing as well as the other experiments. Overall, the best experiment is AMMABC, which is consistent with what has already been observed in terms of TCWV and averaged precipitation amounts. A finer analysis of daily performance was focused on a Sahel zone (10°–20°N, 10°W–10°E). Daily amounts of precipitation are presented in Fig. 10. Again, the NOAMMA experiment produces rain variability that is not in agreement with the observed data. All of the other experiments match quite closely the daily variations, with a clear advantage for AMMABC.

In this paragraph, the 24-h precipitation ending at 0600 UTC 11 August 2006 is used to present the positive impacts of the humidity bias correction, and the use of soundings with a large number of vertical levels on the daily precipitation forecasts. Observations from FEWS NET based on satellite and rain gauge data

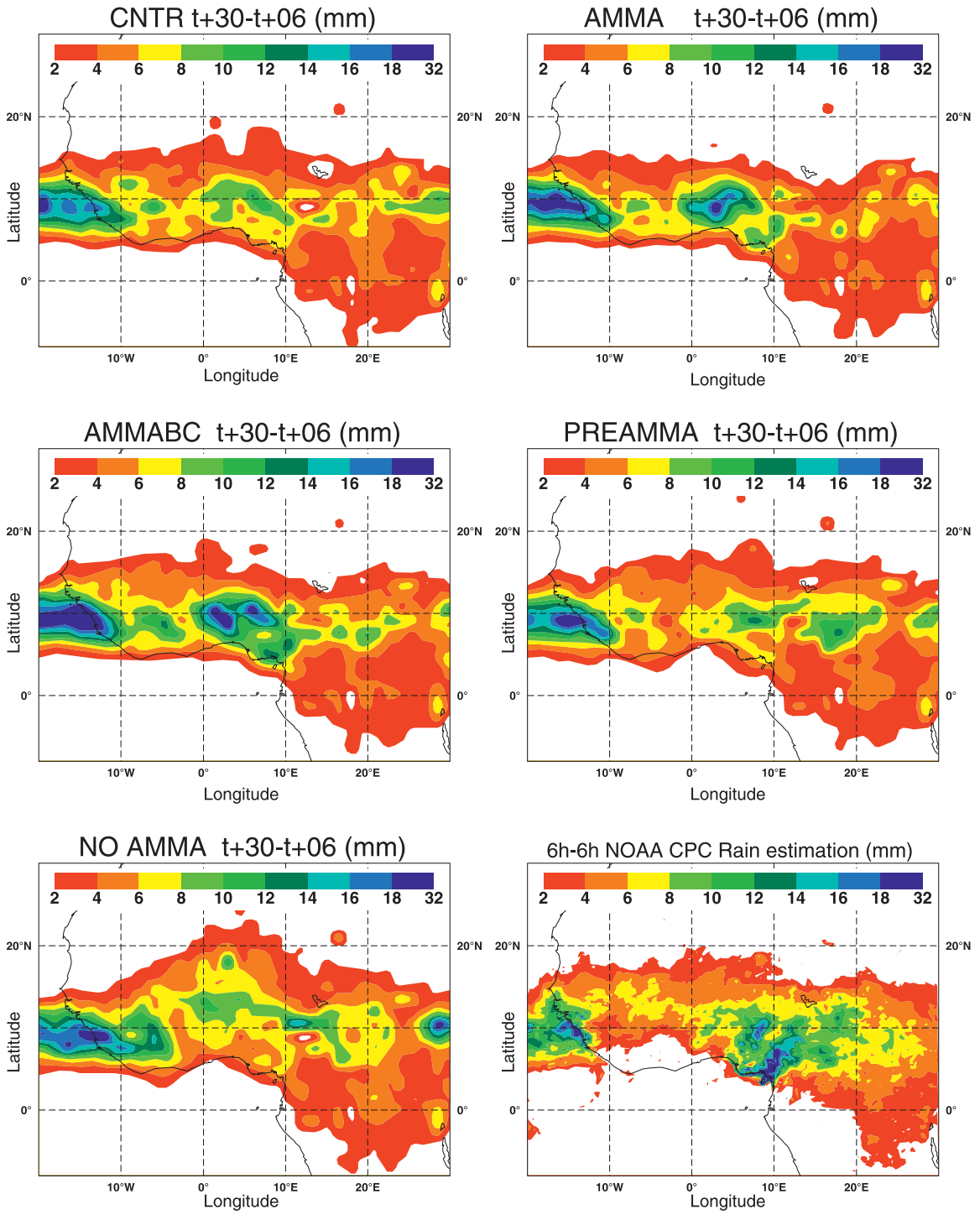

FIG. 8. The 24-h mean precipitation (from $t + 6$ to $t + 30$) during August 2006 for (top left) CNTR, (top right) AMMA, (middle left) AMMABC, (middle right) PREAMMA, and (bottom left) NOAMMA. (bottom right) The rainfall estimation (mm) from FEWS NET is based on satellite and rain gauge data.

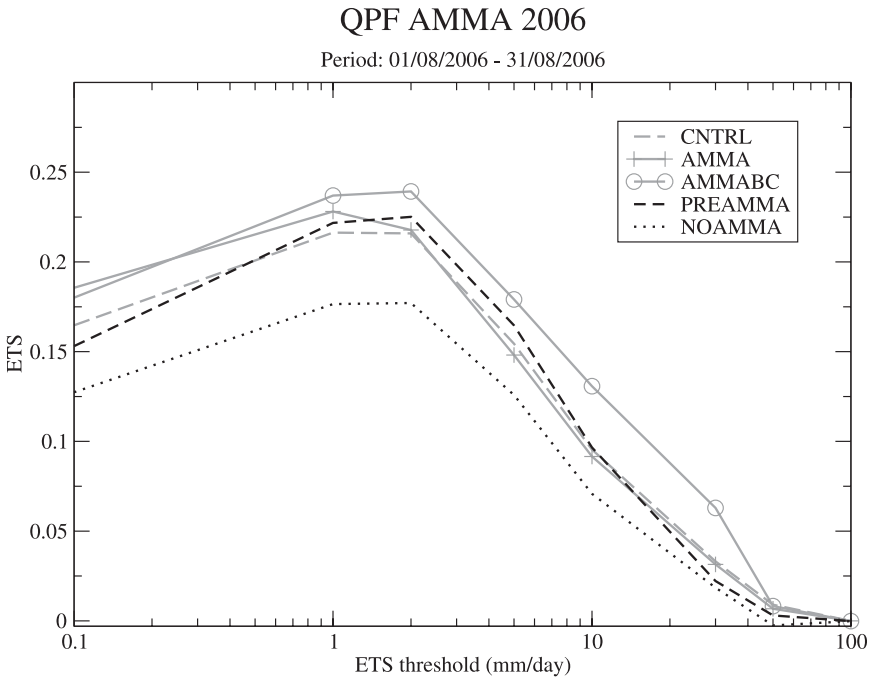

FIG. 9. ETSs, averaged over August 2006, for various assimilation experiments. The verification is provided by the FEWS NET based on satellite and rain gauge data.

(Fig. 11, bottom right) show several areas of high precipitation, with maxima of over 80 mm (dark blue) inland, to the north of the Guinea Gulf. All five experiments reproduce the rainfall over the sea and across the southwestern African border. However, only the experiments using all the soundings from the 2006 network (CNTR, AMMA, and AMMABC) are able to correctly reproduce the precipitation to the north of the Guinea

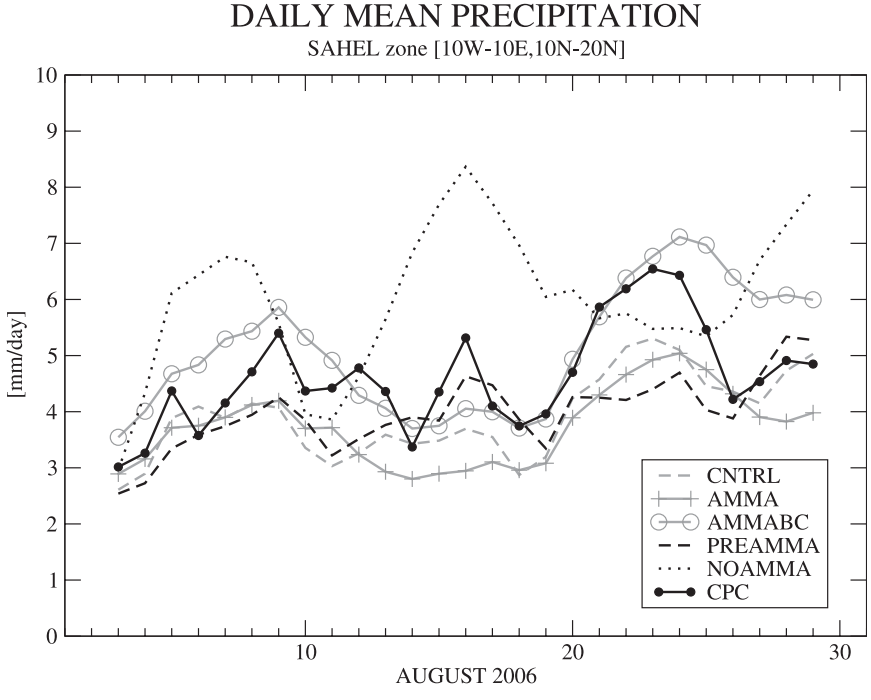

FIG. 10. Daily precipitation averaged over a Sahelian region, for the various assimilation experiments and the FEWS NET reference.

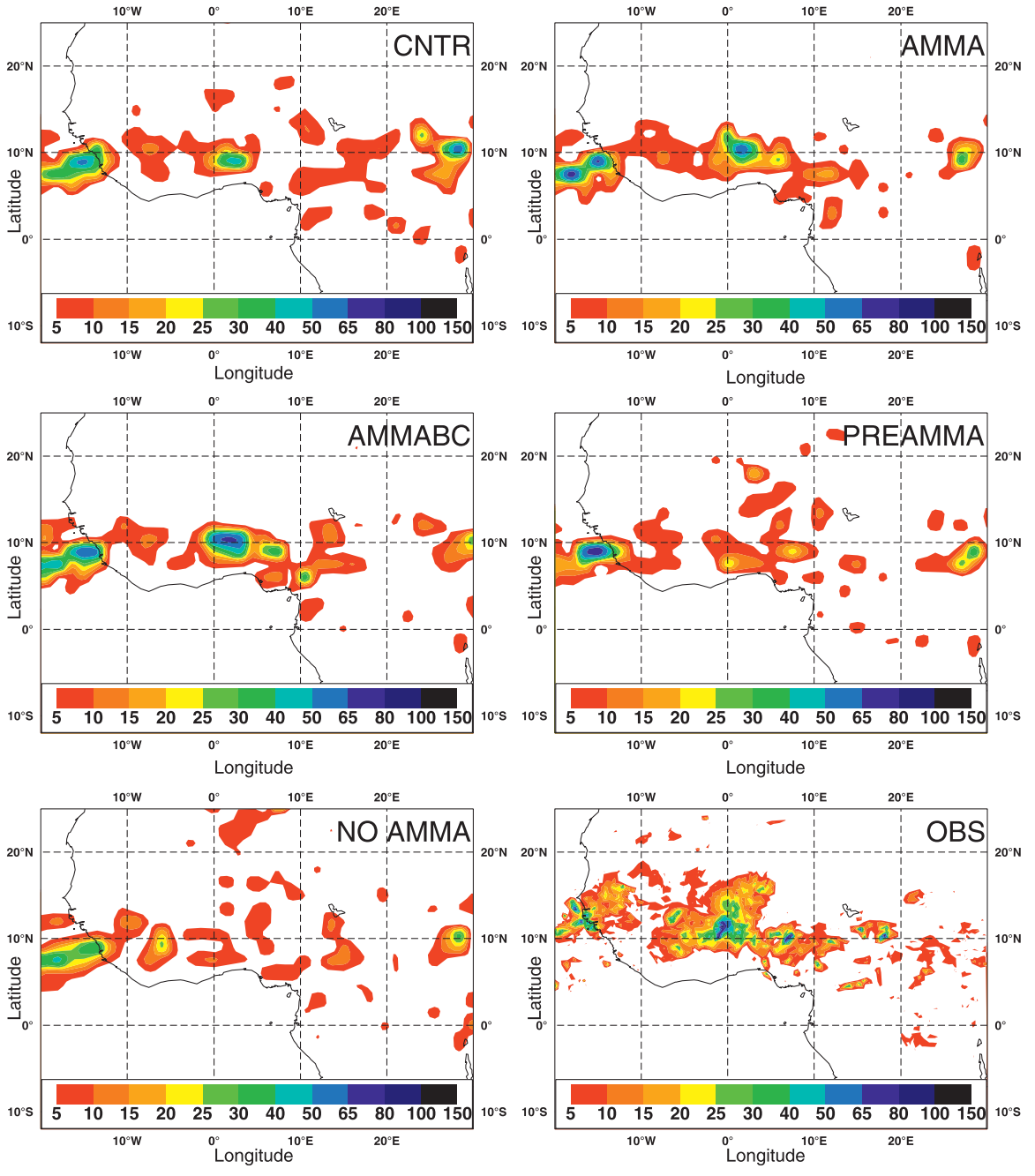

FIG. 11. The 24-h accumulated precipitation (mm) ending at 0600 UTC 11 Aug 2006 for (a) CNTR, (b) AMMA, (c) AMMABC, (d) PREAMMA, (e) NOAMMA, and (f) estimated from FEWS NET based on satellite and rain gauge data.

Gulf, even if the horizontal extent of the rainfall area is underestimated. CNTR (Fig. 11, top left) reproduces only the position of the larger maximum, but not the amount of precipitation. AMMA (Fig. 11, top right) increases this maximum compared to CNTR, but it is lower than observed. Nevertheless, AMMA presents a second maximum to the right of the main one, in agreement with the observations. AMMABC (Fig. 11, middle left) correctly reproduces the position and the value of the main maximum and partially increases the second one, but still less than the amounts observed. PREAMMA (Fig. 11, middle right) clearly misses the forecast for 11 August 2006, underestimating the precipitation everywhere inland and even missing the structure of the system. As for NOAMMA (Fig. 11, bottom left), it fails to provide any relevant information on the inland precipitation for that day.

TABLE 4. Averaged means (M) and std devs (STD) of the differences between model fields at various forecast ranges and SYNOP surface observations for SLP, RH, speed and wind direction (FF and DD), cloud cover, and temperature (T). Scores were computed for the period 15 Jul–15 Sep 2006.

Expt	SLP (hPa)		RH (%)		FF (m s^{-1})		DD (°)		Cloud cover (octas)		T (°C)	
$t + 0$	M	STD	M	STD	M	STD	M	STD	M	STD	M	STD
CNTR	0.67	1.48	−3.54	17.16	0.41	2.46	2.48	54.73	−1.91	33.57	0.40	2.16
AMMA	0.63	1.46	−3.89	17.31	0.38	2.43	1.67	54.81	−1.90	33.77	0.40	2.14
AMMABC	0.62	1.46	−2.15	16.73	0.37	2.43	2.60	54.49	−0.33	32.78	0.34	2.14
PREAMMA	0.68	1.48	−3.31	17.04	0.43	2.47	2.91	54.03	−1.93	33.15	0.36	2.14
$t + 24$	M	STD	M	STD	M	STD	M	STD	M	STD	M	STD
CNTR	0.88	1.85	−1.79	17.14	0.54	2.63	2.10	57.06	−1.08	33.07	−0.02	2.53
AMMA	0.82	1.80	−2.15	17.14	0.56	2.64	1.64	56.82	−0.98	33.16	0.01	2.52
AMMABC	0.75	1.79	−0.91	16.97	0.50	2.62	0.98	57.91	0.85	32.33	−0.11	2.53
PREAMMA	0.85	1.82	−1.54	17.13	0.52	2.62	0.36	56.32	−0.39	32.38	−0.04	2.50
$t + 48$	M	STD	M	STD	M	STD	M	STD	M	STD	M	STD
CNTR	0.70	1.90	−1.76	17.39	0.50	2.60	0.96	57.68	−3.04	33.37	−0.01	2.59
AMMA	0.70	1.89	−2.00	17.47	0.52	2.61	0.14	58.18	−4.16	33.31	0.02	2.61
AMMABC	0.65	1.89	−1.05	17.29	0.48	2.60	−0.05	59.06	−1.65	32.33	−0.10	2.63
PREAMMA	0.68	1.87	−1.51	17.40	0.48	2.57	0.09	58.20	−2.92	33.00	−0.03	2.57
$t + 72$	M	STD	M	STD	M	STD	M	STD	M	STD	M	STD
CNTR	0.49	1.97	−2.00	17.64	0.50	2.62	2.67	59.92	−4.58	33.98	0.02	2.65
AMMA	0.52	1.95	−2.37	17.60	0.51	2.63	1.60	59.12	−4.99	33.66	0.07	2.63
AMMABC	0.52	1.95	−1.35	17.59	0.44	2.56	1.91	60.76	−3.26	32.56	−0.07	2.68
PREAMMA	0.47	1.94	−1.49	17.63	0.47	2.59	1.97	59.86	−4.12	33.25	0.00	2.63

b. Impact on forecast performance

Table 4 presents a summary of the scores at four different forecast ranges, during the 2-month period over Africa (north of the equator) for several surface variables: sea level pressure, RH, wind speed and direction, cloud cover, and temperature. At 0-h forecast range, AMMABC has the best results for the comparison with the North African SYNOPs for all of the parameters except for the wind direction. For the other forecast ranges, AMMABC always presents the smallest mean error and standard deviation compared to the other experiments except for temperature and in a few cases. AMMA is, on average, slightly better than CNTR for 0 h and $t + 24$ but CNTR is better for $t + 48$. At 72 h, CNTR obtains smaller biases but AMMA has the smaller standard deviation. Notice that PREAMMA obtains scores that are similar to those of AMMA and CNTR. Significance tests were performed and it was found that AMMABC was significantly better than the other experiments, mainly for the analysis of relative humidity (at the 95% confidence level for the Student's t test). These scores confirm that the AMMABC experiment is on average better for the short range than the other experiments, locally over Africa.

To investigate the potential propagation of this signal to other regions, the difference in the scores between AMMABC and PREAMMA was computed for the period 1 August–14 September 2006. Results are displayed in Figs. 12–14 for the geopotential at 500 hPa at forecast ranges of 24, 48, and 72 h. Blue-shaded areas indicate where AMMABC improves the forecast over the PREAMMA experiment. The small improvement noticed over Africa at the 24-h range (Fig. 12) clearly propagates to the west and north to reach Europe at 48- and 72-h ranges (Figs. 13 and 14). One should note, however, that these results are not statistically significant. The westward propagation over Africa seems to be linked to easterly waves. As we have seen, the experiments using additional radiosondes extend the AEJ to the south, which can enhance African easterly waves, as shown in Leroux and Hall (2009). The subsequent propagation to the north can probably be linked to Rossby waves and is consistent with other studies in which the characteristics of the African monsoon have been shown to influence Europe (Bielli et al. 2008, manuscript submitted to *Climate Dyn.*; Cassou et al. 2005). It then appears that the enhancement of the radiosonde network over Africa has a downstream positive impact at higher latitudes after a couple of days

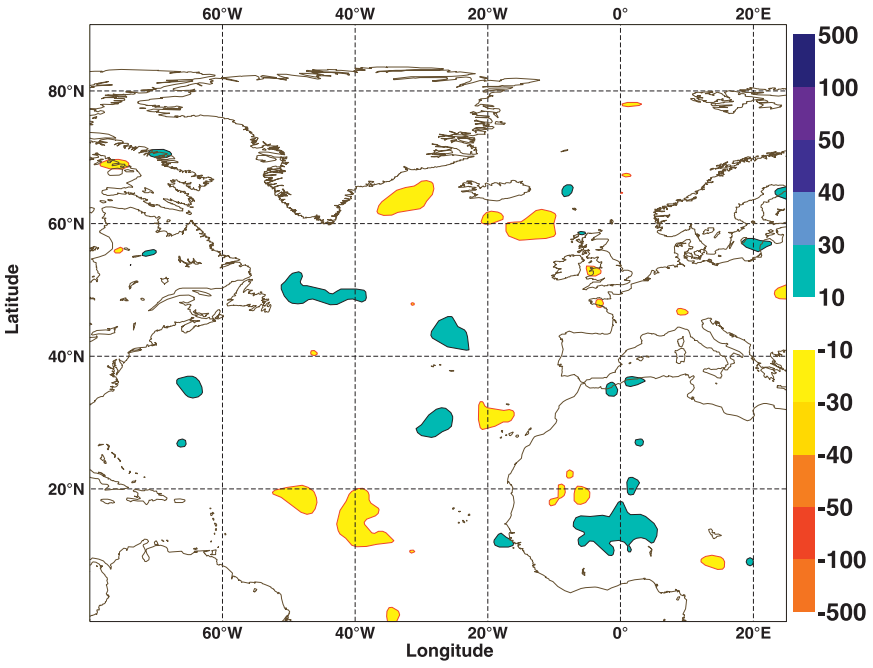

FIG. 12. Differences in RMS errors (m) between the AMMABC and PREAMMA forecasts. The errors are computed with respect to the ECMWF analysis, for the geopotential at 500 hPa at 24-h range, over the period 1 Aug–14 Sep 2006.

in the forecast. This is confirmed by looking at scores with respect to radiosonde observations over Europe. Figure 15 shows the forecast errors for geopotential, temperature, humidity, and wind at 3-day range with respect to radiosonde data over Europe, for the PREAMMA (in black) and AMMABC (in gray) experiments. There is a clear improvement in forecast performance over the whole atmosphere in both bias and root-mean

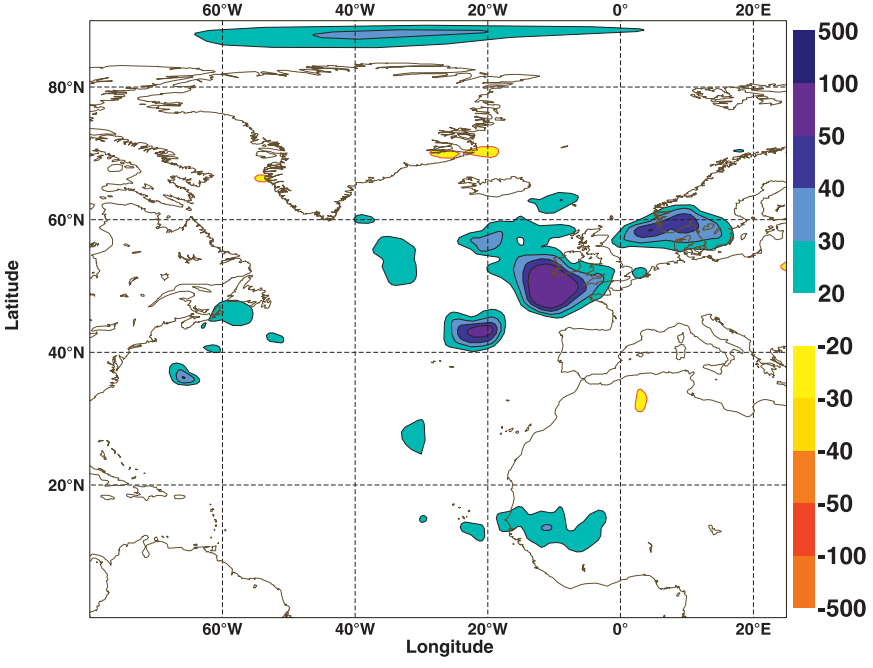

FIG. 13. Differences in RMS errors (m) between the AMMABC and PREAMMA forecasts. The errors are computed with respect to the ECMWF analysis, for the geopotential at 500 hPa at 48-h range, over the period 1 Aug–14 Sep 2006.

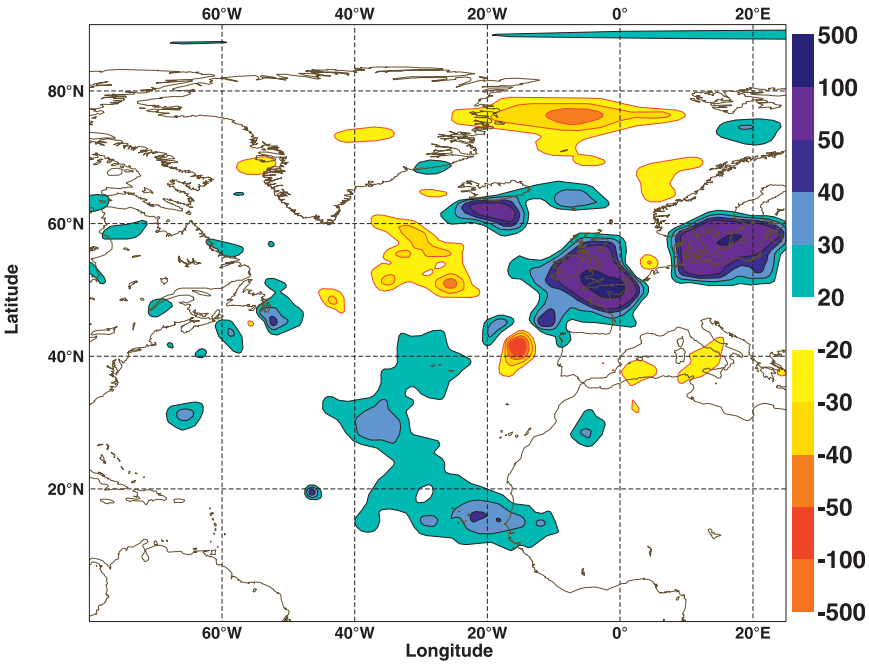

FIG. 14. Differences in RMS errors (m) between the AMMABC and PREAMMA forecasts. The errors are computed with respect to the ECMWF analysis, for the geopotential at 500 hPa at 72-h range, over the period 1 Aug–14 Sep 2006.

square when AMMA data are assimilated for the geopotential field (results are statistically significant at most levels in the atmosphere). This result also holds for the RMS error of the temperature from the surface to 500 hPa (not significant), of the humidity between 700 and 400 hPa (statistically significant at 700 hPa), and of the wind in the troposphere (statistically significant at 200 hPa).

6. Conclusions

The aim of this study was to assess the changes produced in the forecast by the special soundings recorded during the 2006 African Monsoon Multidisciplinary Analysis campaign. These data, which present many more vertical levels than a standard WMO radiosonde, were used to initialize ARPEGE 4DVAR with a 6-h assimilation window. Four different experiments were performed during the 2 months of the intense phase of the monsoon (from mid-July to mid-September). Their different configurations were designed to evaluate the model's sensitivity to 1) the increased number of vertical levels, 2) the humidity bias correction, and 3) the distribution of the radiosonde stations over western Africa. Furthermore, an additional experiment was run for 45 days, removing all AMMA radiosonde observations.

Results have shown that the increase in the number of observations was not as positive as could have been expected, if not accompanied by a proper processing of the observations. The impact of these soundings was largely improved if a bias correction was applied to the relative humidity measurements. It is worth mentioning that the results of these impacts of the bias correction are consistent with similar AMMABC versus AMMA experiments performed using the ECMWF model (Agusti-Panareda et al. 2009). The removal of the dry bias, affecting data coming from several radiosondes used for the 2006 campaign, positively impacted our humidity analyses, scores, and precipitation fields. A remarkable reduction in the mean error of the surface relative humidity was observed up to $t + 72$, and other surface variables were in general better than in the reference experiment. The TCWV was largely increased inland along the African coasts, and the 24-h precipitation was in good agreement with the observations. The comparison between the network distribution in 2005 and 2006 showed that the additional radiosondes to the south of 10° south increased the AEJ on its southeasterly side. A comparison with independent GPS data over Africa and precipitation scores shows a clear advantage in the experiment using all AMMA data and a bias correction. On the contrary, the experiment without any AMMA observations is of noticeably poorer quality.

One might wish to go further in the analysis of these results by investigating which particular radiosondes or which particular sets of radiosondes provide the largest

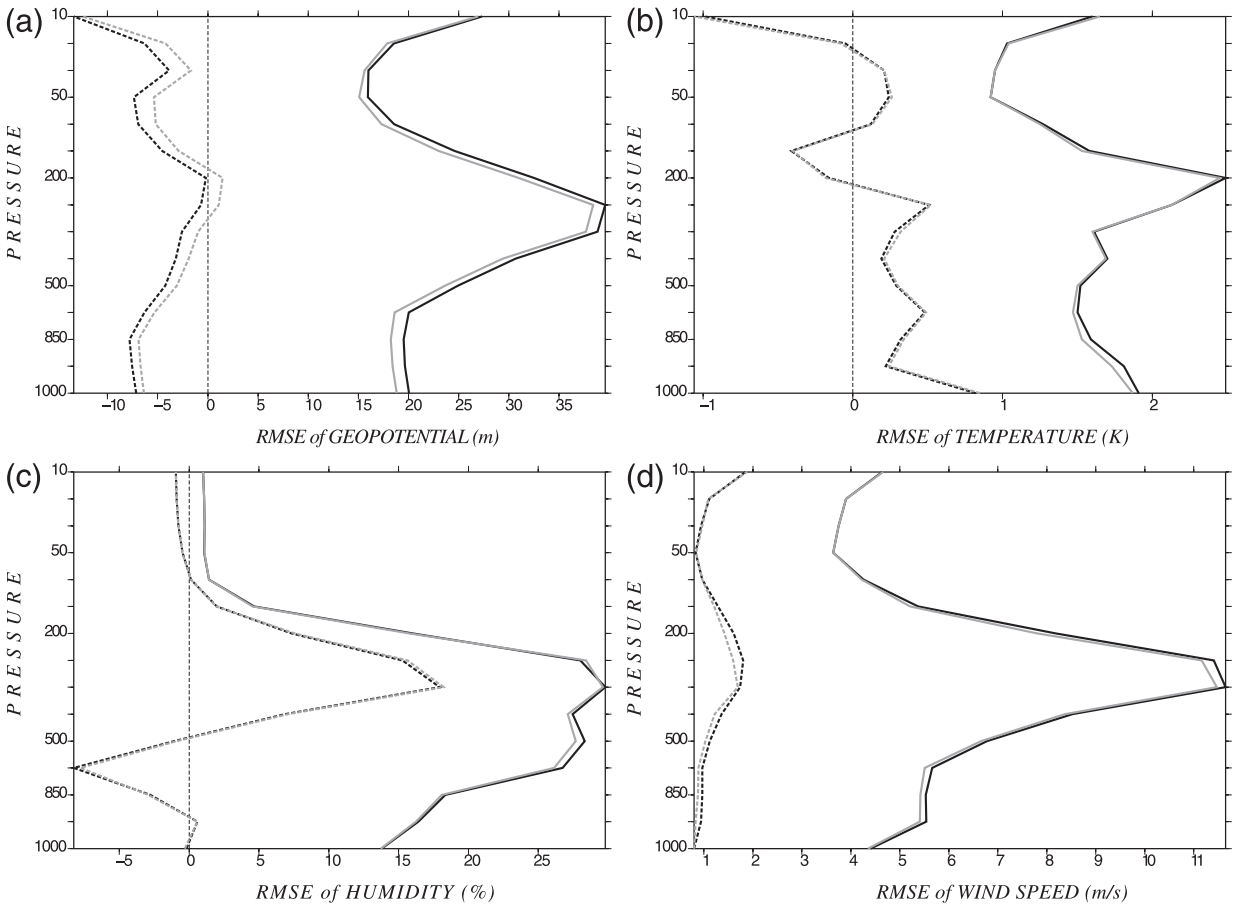

FIG. 15. RMS and mean (BIAS) of the (a) geopotential differences, (b) temperature, (c) humidity, and (d) wind between 72-h forecasts and radiosonde observations for experiments AMMABC (gray) and PREAMMA (black) as a function of pressure. The RMS and mean are represented by solid and dashed lines, respectively. Statistics are calculated over the European region and averaged over the period 1 Aug–14 Sep 2006.

analysis changes and/or forecast improvements. It would be interesting to know, for example, if certain radiosonde stations are more valuable than others. The impact of individual observations on the analysis can be measured by the degrees of freedom for signal (DFSs), which quantifies the sensitivity of the analysis estimated in the observation space with respect to the observations (Cardinali et al. 2004; Chapnik et al. 2006). This diagnostic was thought to be useful for assessing the contribution to the analysis of each radiosonde in the 2006 network, and computations were performed for the first 2 weeks in August. However, the interpretation of the results was difficult because of the large differences in the numbers of individual data points collected at each radiosounding site. It was found that soundings with a large number of vertical levels, a high temporal frequency of availability, and with a relatively dense horizontal distribution, such as in 2006, reduced the contribution of each individual datum to the analysis, because of the higher level of redundancy among their data. Despite these caveats, one comparison could be made between the Bamako, Mali, and Ouagadougou, Burkina Faso, stations, due to a similar number of observations and a similar observation frequency. Bamako is located at 12° latitude and −8° longitude and Ouagadougou at 12° latitude and −2° longitude. It was found that Bamako had a larger DFS than Ouagadougou. This can be explained by the geographical location of Bamako, which is quite isolated, unlike Ouagadougou, which is close to Tamale, Ghana; Djougou, Benin; and Niamey. The link between DFS and observation density was also found by Fourrié et al. (2006). In any case, globally, it was found that the AMMA radiosonde stations strongly controlled the analysis of the systems. One could probably use other diagnostics such as the sensitivity of the forecast to the observations (Langland and Baker 2004; Cardinali 2009) to obtain a more in-depth analysis, but these tools were not available for this study.

The improvements due to the AMMA data over Africa are shown to propagate downstream and reach Europe after a couple of days in the forecast. In conclusion, although the results obtained in this study should be confirmed over longer periods, these experiments have highlighted the need for an accurate processing of the humidity data over the West African region and the large potential benefit to be gained by increasing the number of observations in this area, both for local forecasts and for downstream impacts.

Acknowledgments. Three anonymous reviewers are acknowledged for their numerous and insightful comments, which helped to improve the manuscript. The authors express their thanks to Laurence Fleury for her technical help with the AMMA database. We would also like to acknowledge Jean Maziejewski, Vincent Guidard, Anton Beljaars, and Jean-Luc Redelsperger for their help, comments, and advice on this work. Based on a French initiative, AMMA was built by an international scientific group and is currently funded by a large number of agencies, especially from France, the United Kingdom, the United States, and Africa. This project has been the recipient of an important financial contribution from the European Community's Sixth Framework research program. Detailed information on scientific coordination is available on the AMMA international Web site (http://www.amma-international.org).

REFERENCES

Agusti-Panareda, A., and A. Beljaars, 2008: ECMWF's contribution to AMMA. *ECMWF Newsletter,* No. 115, Reading, United Kingdom, 19–27.

——, and Coauthors, 2009: Radiosonde humidity bias correction over West African region for the special AMMA reanalysis at ECMWF. *Quart. J. Roy. Meteor. Soc.,* **135,** 595–617.

Berre, L., S. E. Stefánescu, and M. B. Pereira, 2006: The representative of the analysis effect in three error simulation techniques. *Tellus,* **58A,** 196–209.

Bock, O., M.-N. Bouin, A. Walpersdorf, J. Lafore, F. Guichard, and A. Agusti-Panareda, 2007: Comparison of ground-based GPS precipitable water vapour to independent observations and NWP model reanalyses over Africa. *Quart. J. Roy. Meteor. Soc.,* **133,** 2011–2027.

——, and Coauthors, 2008: The West African monsoon observed with ground-based GPS receivers during AMMA. *J. Geophys. Res.,* **113,** D21105, doi:10.1029/2008JD010327.

Bouttier, F., F. Lalaurette, B. Norris, and D. Vasiljevic, 1999: Reimplementation of the TEMP-T bias correction. ECMWF RD and OD Memo, 15 pp.

Cardinali, C., 2009: Monitoring the observation impact on the short-range forecast. *Quart. J. Roy. Meteor. Soc.,* **135,** 239–250.

——, S. Pezzuli, and E. Andersson, 2004: Influence matrix diagnostic of a data assimilation system. *Quart. J. Roy. Meteor. Soc.,* **130,** 2767–2786.

Cassou, C., L. Terray, and A. S. Phillips, 2005: Tropical Atlantic influence on European heat waves. *J. Climate,* **18,** 2805–2811.

Chapnik, B., G. Desroziers, F. Rabier, and O. Talagrand, 2006: Diagnosis and tuning of observational error in a quasi-operational data assimilation setting. *Quart. J. Roy. Meteor. Soc.,* **132,** 543–565.

Courtier, P., C. Freydier, J.-F. Geleyn, F. Rabier, and M. Rochas, 1991: The ARPEGE Project at Météo-France. *Proc. Workshop on Numerical Methods in Atmospheric Modelling,* Vol. 2, Reading, United Kingdom, ECMWF, 193–231.

——, J.-N. Thépaut, and A. Hollingsworth, 1994: A strategy for operational implementation of 4D-Var, using an incremental approach. *Quart. J. Roy. Meteor. Soc.,* **120,** 1367–1387.

Fourrié, N., D. Marchal, F. Rabier, B. Chapnik, and G. Desroziers, 2006: Impact study of the 2003 North Atlantic THORPEX regional campaign. *Quart. J. Roy. Meteor. Soc.,* **132,** 275–295.

Gauthier, P., and J.-N. Thépaut, 2001: Impact of the digital filter as a weak constraint in the pre-operational 4DVAR assimilation system of Météo-France. *Mon. Wea. Rev.,* **129,** 2089–2102.

Grody, N., 1998: Surface identification using satellite microwave radiometers. *IEEE Trans. Geosci. Remote Sens.,* **26,** 850–859.

Janisková, M., J.-N. Thépaut, and J. Geleyn, 1999: Simplified and regular physical parametrizations for incremental four-dimensional variational assimilation. *Mon. Wea. Rev.,* **127,** 26–45.

Karbou, F., E. Gérard, and F. Rabier, 2006: Microwave land emissivity and skin temperature for AMSU-A and -B assimilation over land. *Quart. J. Roy. Meteor. Soc.,* **132,** 2333–2355.

——, ——, and ——, 2009a: Global 4DVAR assimilation and forecast experiments using land surface emissivities from AMSU-A and AMSU-B observations. Part I: Impact on sounding channels. *Wea. Forecasting,* in press.

——, F. Rabier, J.-P. Lafore, J.-L. Redelsperger, and O. Bock, 2009b: Global 4DVAR assimilation and forecast experiments using land surface emissivities from AMSU-A and AMSU-B observations. Part II: Impact of adding surface channels on the African monsoon during AMMA. *Wea. Forecasting,* in press.

Langland, R., and N. Baker, 2004: Estimation of observation impact using the NRL atmospheric variational data assimilation adjoint system. *Tellus,* **56A,** 189–201.

Laws, K. B., J. E. Janowiak, and G. J. Huffman, 2004: Verification of rainfall estimates over Africa using RFE, NASA MPA-RT, and CMORPH. Preprints, *18th Conf. on Hydrology,* Seattle, WA, Amer. Meteor. Soc., P2.2. [Available online at http://ams.confex.com/ams/pdfpapers/67983.pdf.]

Leroux, S., and N. Hall, 2009: On the relationship between African easterly waves and the African easterly jet. *J. Atmos. Sci.,* **66,** 2303–2316.

Lorenc, A., D. Barker, R. Bell, B. Macpherson, and A. Maycock, 1996: on the use of radiosonde humidity observation in middle latitude NWP. *Meteor. Atmos. Phys.,* **60,** 3–17.

Milesi, C., H. Hashimoto, S. Running, and R. Nemani, 2005: Climate variability, vegetation productivity and people at risk. *Global Planet. Change,* **47,** 221–231.

Nuret, M., J. Lafore, O. Bock, F. Guichard, A. Agusti-Panareda, J.-B. N'Gamini, and J.-L. Redelsperger, 2008: Correction of humidity bias for Vaisala RS80-A sondes during AMMA 2006 observing period. *J. Atmos. Oceanic Technol.,* **25,** 2152–2158.

Parker, D. J., and Coauthors, 2005: The diurnal cycle of the West African monsoon circulation. *Quart. J. Roy. Meteor. Soc.,* **131,** 2839–2860.

——, and Coauthors, 2008: The AMMA radiosonde program and its implications for the future of atmospheric monitoring over Africa. *Bull. Amer. Meteor. Soc.,* **89,** 1015–1027.

Rabier, F., H. Järvinen, E. Klinker, J.-F. Mahfouf, and A. Simmon, 2000: The ECMWF operational implementation of four-dimensional variational assimilation. I: Experimental results with simplified physics. *Quart. J. Roy. Meteor. Soc.,* **126,** 1143–1170.

Redelsperger, J.-L., C. D. Thorncroft, A. Diedhiou, T. Lebel, D. J. Parker, and J. Polcher, 2006: African Monsoon Multidisciplinary Analysis: An international research project and field campaign. *Bull. Amer. Meteor. Soc.,* **87,** 1739–1746.

Roy, B., J. Halverson, and J. Wang, 2004: The influence of radiosonde age on TRMM field campaign soundings humidity correction. *J. Atmos. Oceanic Technol.,* **21,** 117–132.

Sultan, B., C. Baron, M. Dingkuhn, B. Sarr, and S. Janicot, 2005: Agricultural impacts of large-scale variability of the West African monsoon. *Agric. For. Meteor.,* **128,** 93–110.

Veersé, F., and J.-N. Thépaut, 1998: Multiple-truncation incremental approach for four-dimensional variational data assimilation. *Quart. J. Roy. Meteor. Soc.,* **124,** 1889–1908.

Wang, J., H. L. Cole, D. Carlson, E. Miller, and K. Beierle, 2002: Correction of humidity measurements error from Vaisala R80 radiosonde—Application to TOGA COARE data. *J. Atmos. Oceanic Technol.,* **19,** 981–1002.

Weng, F., B. Yan, and N. Grody, 2001: A microwave land emissivity model. *J. Geophys. Res.,* **106** (D17), 20 115–20 123.